Study of the parametric oscillator driven by narrow-band noise to model the response of a fluid surface to time-dependent accelerations

Wenbin Zhang, Jaume Casademunt, and Jorge Viñals
Supercomputer Computations Research Institute, B-186 Florida State University, Tallahassee, Florida 32306-4052

(Received 29 December 1992; accepted 19 August 1993)

A stochastic formulation is introduced to study the large amplitude and high-frequency components of residual accelerations found in a typical microgravity environment (or *g*-jitter). The linear response of a fluid surface to such residual accelerations is discussed in detail. The analysis of the stability of a free fluid surface can be reduced in the underdamped limit to studying the equation of the parametric harmonic oscillator for each of the Fourier components of the surface displacement. A narrow-band noise is introduced to describe a realistic spectrum of accelerations, that interpolates between white noise and monochromatic noise. Analytic results for the stability of the second moments of the stochastic parametric oscillator are presented in the limits of low-frequency oscillations, and near the region of subharmonic parametric resonance. Based upon simple physical considerations, an explicit form of the stability boundary valid for arbitrary frequencies is proposed, which interpolates smoothly between the low frequency and the near resonance limits with no adjustable parameter, and extrapolates to higher frequencies. A second-order numerical algorithm has also been implemented to simulate the parametric stochastic oscillator driven with narrow-band noise. The simulations are in excellent agreement with our theoretical predictions for a very wide range of noise parameters. The validity of previous approximate theories for the particular case of Ornstein–Uhlenbeck noise is also checked numerically. Finally, the results obtained are applied to typical microgravity conditions to determine the characteristic wavelength for instability of a fluid surface as a function of the intensity of residual acceleration and its spectral width.

I. INTRODUCTION

Faraday waves arise when the free surface of a fluid is parametrically excited by an oscillatory external force (for a recent review see, e.g., Ref. 1). We study in this paper the linear response of a free surface when the fluid is driven by an external *random* force perpendicular to the quiescent fluid surface. A narrow-band stochastic process is introduced as a model for the external force that allows a systematic study from a white noise limit (in which the driving force has no preferred frequency component), to a process characterized by a very narrow frequency spectrum, and hence approaching the limit of a periodic external force.

In the classical case, a layer of fluid is driven by an external force normal to the free surface at rest. Small displacements of the surface away from planarity can be described by the equation of the parametric harmonic oscillator.[2] When the external force is sinusoidal in time, this equation reduces to the classical Mathieu equation. Parametric resonance is obtained when the natural frequency of the oscillator is close to a multiple of half the frequency of the external force. More recent studies of this system have focused on the nonlinear regime, and have addressed the appearance and evolution of spatial patterns following the instability of the planar surface, and on secondary instabilities of those patterns.[3–7] Other examples of parametric resonance phenomena modeled by the Mathieu equation can be found in different contexts, including for instance, the study of acoustic instabilities in premixed flames,[8] the onset of Rayleigh–Bénard convection under oscillatory accelerations,[9,10] or modulated thermosolutal convection during directional solidification.[11]

We focus our attention in this paper on surface waves, but consider instead an external driving force that is a *random* function of time. Our approach is motivated by the significant levels of residual accelerations that have been detected during space missions in which microgravity experiments were being conducted.[12–14] We note, however, that our analysis also encompasses other experimental situations in which the external driving force is not monochromatic. The residual acceleration field can be decomposed for practical purposes into two contributions: $\mathbf{g}_s$ and $\mathbf{g}(t)$, where $\mathbf{g}_s$ denotes a quasisteady or systematic component (either constant or changing very slowly in time), and $\mathbf{g}(t)$ denotes a fluctuating contribution (sometimes called *g*-jitter), which averages to zero. The variety of sources contributing to $\mathbf{g}_s$ will not be discussed here. It is sufficient for our purposes to note that typical values of $\|\mathbf{g}_s\|$ are around $10^{-6} g_E$ (g_E is the gravitational field on the Earth's surface) and characteristic frequencies are lower than 10^{-2} Hz.[13,15] The fluctuating contribution $\mathbf{g}(t)$ is thought to be of a statistical nature. Characteristic frequencies of *g*-jitter are 1 Hz or higher, and their amplitude is typically two or three orders of magnitude larger than the quasisteady component. We will assume in this work that $\mathbf{g}(t)$ is a random function of time, to be defined below.

Most previous theoretical analyses of the effect of *g*-jitter on a variety of fluid problems have been restricted to modeling the high-frequency component of the residual

 0899-8213/93/5(12)/3147/15/$6.00

acceleration as a periodic function of time, or as isolated pulses of short duration. Jacqmin and Duval[16] studied the instabilities of the interface between two immiscible, viscous fluids caused by oscillatory accelerations, extending the classical case that involves a free surface only. Jacqmin further extended this study to a fluid layer with a uniform density gradient and explicitly considered components of the gravity vector parallel and normal to the density gradient.[17] The sensitivity of liquid bridges to axial oscillatory accelerations has also been addressed.[18,19] The results show that the response of the surface of the bridge is essentially an ordinary (nonparametric) resonance phenomenon, in which the amplitude of the oscillations is largest around the natural frequencies of the bridge. The effect of residual accelerations of oscillatory nature on buoyancy-driven convection has been studied by Alexander *et al.*[20] and Wheeler *et al.*[10] In the former case, the configuration analyzed is appropriate for Bridgman crystal growth from the melt. Unsteady residual accelerations are seen to lead to unsteady convection in the melt, which in turn results in composition inhomogeneities in the solid. In the second work, the authors investigate the onset of a convective instability in fluid configurations appropriate for directional solidification and Rayleigh–Bénard convection under oscillatory residual accelerations. Interestingly, the linear stability analysis of the stress-free Rayleigh–Bénard problem also reduces to the damped Mathieu equation.[9]

Although a certain amount of attention has been paid to modeling the high-frequency components of g-jitter as periodic functions of time, little has been done to address the more realistic case of a driving force that contains a band of frequencies, and that is of a random nature. Early attempts in this direction by Antar,[21] considered the stability of the Rayleigh–Bénard configuration under a random gravitational field. His analysis in effect led to the equation of the parametric harmonic oscillator. He considered a random external force, uncorrelated in time (white noise), and studied the stability of the fluid layer. The results which we describe below reduce to his in the limit of white noise. In later work, Fichtl and Holland[22] studied the probability that gravitational impulses would exceed a certain threshold and duration. They considered a generic random process defined by its power spectrum, and described specific results for the case of the Ornstein–Uhlenbeck process.

Each spatial Fourier mode of the free surface displacement in a slightly viscous fluid satisfies the equation of a damped parametric harmonic oscillator in the linear regime. This equation, for example, follows directly from the equations of the quasipotential approximation.[23] We focus in this paper on an analytic and numerical study of the parametric oscillator with a random frequency. A narrow-band noise is introduced to study the region between the white noise limit and the classical, periodic case. The white noise case is discussed with some detail, complementing known results with the study of the first passage time statistics. For the general case of narrow-band noise the regime of stability of the mean-squared displacement of the interface is obtained analytically both when the natural frequency of the oscillator is much smaller than the dominant frequency of the external force, and in the vicinity of the subharmonic resonance. We next introduce an analytic formula for the neutral stability curve of the mean-squared displacement that extrapolates these results to the regions of intermediate and high frequencies, where no analytical approximation scheme is available. A numerical algorithm is then implemented to simulate the stochastic parametric oscillator and is used to obtain the complete curve of stability of the mean-squared displacement. The numerical calculations are in excellent agreement with the analytic predictions in the appropriate limits, and with the proposed formula for other frequencies. Other existing theories for the particular case of a Gaussian, nonwhite (Ornstein–Uhlenbeck) noise are also checked numerically. Finally, the implications of our findings on the limits of stability of a fluid surface under typical microgravity conditions are discussed.

II. PROBLEM FORMULATION

Consider an incompressible fluid of density ρ, initially occupying the semi-infinite half-space: $z<0$ and $-\infty<x$, $y<\infty$, and a fluid with negligible density occupying the other half-space. We assume a constant background gravitational field $\mathbf{g}_s=-g_0\hat{k}$, where $\hat{k}$ is the unit vector in the z direction. We also assume that the fluid is weakly viscous, such that the thickness of the viscous boundary layer at the free surface, which is of the order of $\sqrt{\nu/\omega}$, is much smaller than the characteristic wavelength, $2\pi/q$, of the surface wave. Here, $1/\omega$ is the characteristic time scale of oscillation and q is the characteristic wave number. In this underdamped limit ($\nu q^2 \ll \omega$), one can derive quasipotential equations by neglecting high-order viscous damping effects.[23] The linearized quasipotential equations are

$$\nabla^2\phi=0, \quad \text{for } z<0, \tag{1}$$

$$\left.\begin{aligned} &\frac{\partial\phi}{\partial t}+[g_0-g_z(t)]h+2\nu\frac{\partial^2\phi}{\partial z^2}-\Gamma\nabla^2 h=0,\\ &\frac{\partial h}{\partial t}=\frac{\partial\phi}{\partial z}+W,\\ &\frac{\partial W}{\partial t}=-2\nu\frac{\partial^3\phi}{\partial z^3}, \end{aligned}\right\} \quad \text{at } z=0, \tag{2}$$

$$\frac{\partial\phi}{\partial z}\to 0, \quad \text{as } z\to-\infty, \tag{3}$$

where $\phi(x,y,z,t)$ is the potential for the irrotational component of the fluid velocity, $W(x,y,z,t)$ is the z component of the rotational part of the fluid velocity, $h(x,y,t)$ is the interface displacement away from planity, given by $z=h(x,y,t)$, the surface tension, and ν is the kinematic viscosity of the fluid. The fluctuating component of the residual acceleration is assumed to be in the z direction and modeled as a stochastic process with,

$$\langle g_z\rangle=0, \tag{4}$$

$$\langle g_z(t)g_z(t')\rangle=G^2e^{-|t-t'|/\tau}\cos\Omega(t-t'). \tag{5}$$

The Fourier transform of Eq. (5) yields the power spectrum we assume for g-jitter. In this case it is given by two Lorentzians peaked at $\pm\Omega$ and with width τ^{-1}.

By taking Fourier transform of Eqs. (1) and (2) along the x, y directions and solving the z dependence for each Fourier component of ϕ with the boundary condition (3), we have the desired equation for the two-dimensional Fourier transform, $\hat{h}(\mathbf{q},t)$, of the interface displacement $h(x,y,t)$,

$$\frac{\partial^2\hat{h}}{\partial t^2}+4\nu q^2\frac{\partial\hat{h}}{\partial t}+q[g_0-g_z(t)]\hat{h}+\frac{\Gamma q^3}{\rho}\hat{h}=0. \tag{6}$$

A term proportional to νW has been neglected since it is negligible in the underdamped limit.

Some comments on the validity of the underdamped approximation are needed. A mode $\hat{h}(\mathbf{q},t)$ responds to the external forcing in a time scale that is set in part by the forcing term $g_z(t)$, and that may differ from the natural frequency $\omega_0(q)$ of that mode defined by Eq. (6), with $g_z(t)=0$. If the forcing term contains a broad band of frequencies, the response of $\hat{h}(\mathbf{q},t)$ also contains a multiplicity of time scales. Hence the underdamped condition $\nu q^2 \ll \omega$ should be verified in the entire range of significant frequencies of $\hat{h}(\mathbf{q},t)$. In particular, were the spectrum of the noise very broad, the response of the surface could have components of frequency outside the underdamped range. Only when the range of frequencies of the external force is known, is it possible to determine the range of wave vectors within which the equations for the Fourier modes of the surface displacement are given by Eq. (6).

We note that the general linear stability problem involving an interface separating two immiscible fluids, driven by a time-dependent external force, cannot be reduced to the equation of a parametric harmonic oscillator even in the underdamped limit. The reduction can only be accomplished if the density of one fluid is much smaller than the density of the other fluid. In the general case of two fluids, numerical studies of the full linear stability equations have been done when the external force is sinusoidal in time.[16] When the external force is a random function of time, a numerical solution of a set of stochastic partial differential equations has to be sought, which we defer to future work.

We focus in the present work on the effects of the g-jitter component normal to the quiescent fluid surface. The parallel component leads, to first order, to an additional forcing term in Eq. (6) which vanishes in the limit of an infinite system. Within a linearized treatment, this new term enters the equation additively, as opposed to the multiplicative coupling of $g_z(t)$. It has been shown elsewhere that an additive forcing term does not affect the linear stability of the surface that we discuss in the present work.[24]

III. STOCHASTIC PARAMETRIC OSCILLATOR: STABILITY ANALYSIS

Equation (6) governing the motion of each Fourier component of the interface displacement $\hat{h}(\mathbf{q},t)$ is the equation of the parametric harmonic oscillator with a random frequency. We study in this section the regions of stability of the parametric oscillator when the random component is a narrow-band noise. Specifically, we consider a dynamical variable $x(t)$ that satisfies

$$\ddot{x}+\gamma\dot{x}+[\omega_0^2+\xi(t)]x=0, \tag{7}$$

where $\dot{x}$ denotes the temporal derivative of x and $\xi(t)$ is a random noise to be specified. Contact with Eq. (6) can be made by replacing $x(t)=\hat{h}(q,t)$, $\gamma=4\nu q^2$, $\omega_0^2=g_0q+\Gamma q^3/\rho$ and $\xi(t)=-qg_z(t)$. We wish to study the statistical properties of the variable x in terms of the parameters defining the noise $\xi(t)$. It is well known that the nonlinear coupling between x and $\xi(t)$ may lead to unstable behavior. This phenomenon is known as parametric resonance.

Parametric resonance of the type modeled by Eq. (7) has been widely studied in two limiting cases. When $\xi(t)$ is a sinusoidal function, Eq. (7) reduces to the well-known damped Mathieu equation. When $\xi(t)$ is a Gaussian white noise, there is also a considerable body of literature on the statistical properties of the process $x(t)$. Here we address the more general case in which $\xi(t)$ is a narrow-band process defined by,

$$\xi(t)=S_1(t)\cos\Omega t+S_2(t)\sin\Omega t, \tag{8}$$

where $S_1(t)$ and $S_2(t)$ are two independent and stationary Gaussian processes with zero mean and correlations,

$$\langle S_i(t)S_j(t')\rangle=\langle\xi^2\rangle\delta_{ij}e^{-|t-t'|/\tau},\quad i,\ j=1,\ 2, \tag{9}$$

and τ is a correlation time. The autocorrelation function of $\xi(t)$ is then

$$\langle\xi(t)\xi(t')\rangle=\langle\xi^2\rangle e^{-|t-t'|/\tau}\cos\Omega(t-t'), \tag{10}$$

and the corresponding power spectrum is

$$P(\omega)=\frac{1}{2}\langle\xi^2\rangle\tau\left(\frac{1}{1+\tau^2(\Omega+\omega)^2}+\frac{1}{1+\tau^2(\Omega-\omega)^2}\right). \tag{11}$$

Throughout this paper we normalize the power spectra in such a way that for white noise, with an autocorrelation function given by $\langle\xi(t)\xi(t')\rangle=2D\delta(t-t')$, we have $P(\omega)=D$. A Gaussian white noise can be obtained from narrow-band noise in the limit $\tau\to 0$ with $\langle\xi^2\rangle\tau=D$ (finite). In the particular case of $\Omega=0$, and a finite correlation time τ, also with $\langle\xi^2\rangle=D/\tau$, the resulting $\xi(t)$ is the so-called Ornstein–Uhlenbeck process. In the opposite limit of $\tau\to\infty$ with $\langle\xi^2\rangle$ finite, narrow-band noise reduces to monochromatic noise (see the next section).

If $\xi(t)$ is a stochastic function, the appropriate description of $x(t)$ requires ensemble averages over realizations of the noise $\xi(t)$. Although the stochastic function $\xi(t)$ itself can be decomposed as a superposition of frequency components, the stochastic problem for $x(t)$ is not reducible to the single frequency case because of the nonlinear coupling between the noise variable and the system variable $\xi(t)x(t)$ (multiplicative noise). The equations for averaged quantities such as statistical moments or correlation functions are not in general closed. For instance, averaging Eq. (7) leads to evolution equations for the first moments

of $x(t)$ and $\dot{x}(t)$ which involve the correlation function $\langle x(t)\xi(t)\rangle$. The evolution equation for this correlation function in turn depends on higher-order moments, giving rise to an infinite hierarchy of coupled equations. This is a characteristic feature of nonlinear or linear and multiplicative stochastic differential equations.

Depending on the parameters characterizing both the statistics of the noise and the deterministic components, several truncation schemes can be applied to the hierarchy of equations described above. The equations for the moments of a given order then become closed and linear, and standard stability criteria can be applied to each moment although the stability boundaries sometimes depend on the order of the statistical moments under consideration. Odd moments (in particular first-order moments $\langle x\rangle, \langle\dot{x}\rangle$), are not adequate in general for stability analyses because they may relax to zero even when the system is highly unstable (with even moments diverging exponentially), as a result of cancellations introduced by the ensemble average (in the case at hand because of the fast decay of phase correlations). The physically most relevant moments in the present case are $\langle x^2\rangle$, $\langle x\dot{x}\rangle$ and $\langle\dot{x}^2\rangle$, which are related to the average energy of the oscillations. Therefore, we will discuss in what follows the stability boundary of the stochastic oscillator in terms of the condition that any eigenvalue of the evolution matrix for the second-order moments (to be defined below) has a positive real part.

A. Deterministic limit and monochromatic noise

The deterministic version of Eq. (7) (i.e., $\xi(t)=\xi_0\cos\Omega t$) has been widely studied as an example of parametric instability. For $\xi_0/\Omega^2 \ll 1$, the equation can be studied perturbatively (see Refs. 25 and 26). In the absence of damping and for small enough ξ_0, the solutions are always stable except at resonances: $\omega_0=(n/2)\Omega$, $n=1,2,\ldots$. The strongest resonance occurs at $n=1$, or $\Omega=2\omega_0$. With finite damping γ, there is a finite threshold for resonance. For $n=1$ the critical amplitude for instability is $\xi_0=2\gamma\omega_0$. The neutral stability curve in the neighborhood of the dominant resonance is also known,

$$\frac{\xi_0^2}{4\gamma^2\omega_0^2}=1+\frac{\Omega^2}{\gamma^2}\left(1-\frac{2\omega_0}{\Omega}\right)^2. \tag{12}$$

In order to compare the deterministic limit with our results for narrow-band noise, it is useful to introduce the autocorrelation function $C(t)$ and power spectrum $P(\omega)$ of a deterministic function defined as time averages,[27]

$$C(s)=\lim_{T\to\infty}\frac{1}{T}\int_0^T dt\,\xi(t)\xi(t+s) \tag{13}$$

and

$$P(\omega)=\frac{1}{2}\int_{-\infty}^{\infty} e^{-i\omega s}C(s)ds. \tag{14}$$

If $\xi(t)=\xi_0\cos\Omega t$, one has

$$C(t-t')=\tfrac{1}{2}\xi_0^2\cos\Omega(t-t') \tag{15}$$

and

$$P(\omega)=\frac{\pi}{2}\xi_0^2[\delta(\omega-\Omega)+\delta(\omega+\Omega)]. \tag{16}$$

Equations (15) and (16) are formally equal to the monochromatic limit ($\Omega\tau\to\infty$) of Eqs. (10) and (11) if $\langle\xi^2\rangle=\xi_0^2/2$. Some differences between the two cases remain, however. For monochromatic noise, individual realizations of $\xi(t)$ are sinusoidal functions of time with frequency Ω, but with a random amplitude and phase. Furthermore, the narrow-band noise defined above has a distribution of amplitudes $\psi(\xi)$ that is Gaussian [this is the simplest choice, and it can be justified by invoking the central limit theorem, assuming that there are a large number of noise sources contributing to the process $\xi(t)$]. Consequently, a deterministic forcing and our choice of monochromatic noise are not equivalent, and need not yield the same stability diagram for the parametric oscillator.

Monochromatic noise could be made equivalent to a deterministic forcing by choosing $\psi(\xi)$ to satisfy

$$\psi(\xi)=\tfrac{1}{2}[\delta(\xi-\xi_0)+\delta(\xi+\xi_0)], \tag{17}$$

as we approach the limit $\Omega\tau\to\infty$. We will not pursue this issue further since we are not interested in the limit $\Omega\tau\gg 1$. We point out, however, that when modeling g-jitter as a deterministic and periodic function, some of the consequences that follow from its stochastic nature could be modeled by introducing a distribution of amplitudes and phases of the forcing and the concomitant averages.

B. White and Ornstein–Uhlenbeck noise

A rather complete account of known results on the stochastic parametric oscillator driven by white or Ornstein–Uhlenbeck noise can be found in Ref. 28 and references therein. The white noise limit is the only case in which Eq. (7) can be solved exactly. For Ornstein–Uhlenbeck noise, several approximation schemes have been developed for small τ.[28,29]

A well-known systematic approximation for linear systems of equations with multiplicative noise is a cumulant expansion,[30] in which the expansion parameter is $\sqrt{D\tau}=\tau\sqrt{\langle\xi^2\rangle}$. Let us briefly summarize the steps involved in this approximation scheme. The reader interested in the details is referred to Ref. 30. Consider a system of linear equations of the form,

$$\frac{\partial}{\partial t}u(t)=A_0u(t)+\alpha A_1(t)u(t), \tag{18}$$

where $u(t)$ is a multidimensional array and A_0 and A_1 are two matrices such that A_0 contains the deterministic component of the evolution of $u(t)$, and A_1 the stochastic or fluctuating part. We assume, without loss of generality, that $\langle A_1\rangle=0$. Here α is a parameter that measures the intensity of the fluctuating component. By treating the last term of Eq. (18) as a time-dependent perturbation in the interaction picture, it can be shown that, up to order $\mathcal{O}(\alpha^4\tau^3)$, the ensemble average of u satisfies

$$\frac{\partial}{\partial t}\langle u(t)\rangle=\left[A_0+\alpha^2\int_0^\infty ds\langle A_1(t)e^{sA_0}A_1(t-s)\rangle e^{-sA_0}\right]\times\langle u(t)\rangle. \tag{19}$$

Equation (19) corresponds to the truncation of a cumulant expansion including up to the second cumulant,[30] and becomes exact in the white noise limit $\tau=0$. For Ornstein–Uhlenbeck noise, $\alpha^2=D/\tau$, and the corrections to Eq. (19) are $\mathcal{O}(D^2\tau)$.

For the parametric oscillator, we define the components of the array u as $u_1=\omega_0^2x^2$, $u_2=\omega_0x\dot{x}$ and $u_3=\dot{x}^2$. Equation (7) leads to the set of equations

$$\begin{aligned}\dot{u}_1&=2\omega_0u_2,\\ \dot{u}_2&=-\omega_0u_1-\gamma u_2+\omega_0u_3-\frac{1}{\omega_0}u_2\xi(t),\\ \dot{u}_3&=-2\omega_0u_2-2\gamma u_3-\frac{2}{\omega_0}u_2\xi(t).\end{aligned} \tag{20}$$

The matrix inside the square brackets in Eq. (19) that results from the set of equations (20) can be calculated exactly. The corresponding eigenvalue λ that determines the stability of the second moments in the underdamped limit, $\gamma^2/\omega_0^2\ll1$, has been obtained in Ref. 30,

$$\lambda=-\gamma+\frac{D}{\omega_0^2}\frac{1}{1+(2\omega_0\tau)^2}. \tag{21}$$

For Gaussian white noise, the eigenvalues for the second moments, for $4\omega_0^2\neq\gamma^2$ and arbitrary D, are known exactly,

$$\lambda_1=-\gamma+\frac{4D}{4\omega_0^2-\gamma^2}, \tag{22}$$

$$\lambda_{2,3}=-\gamma-\frac{2D}{4\omega_0^2-\gamma^2}\pm2i\omega_0\sqrt{1-\frac{\gamma^2}{4\omega_0^2}}. \tag{23}$$

Equation (21) reduces to the exact solution for white noise ($\tau\to0$) in the underdamped limit,

$$\lambda=-\gamma+(D/\omega_0^2). \tag{24}$$

In both cases we see that, for a given γ, there is a finite value D above which the second-order moments become unstable.

We finally note that Eq. (24) is also valid for general white noises with non-Gaussian statistics but with nonvanishing higher-order cumulants,[28] and therefore, cannot be obtained as a limit of Ornstein–Uhlenbeck or narrow-band noise. An example of such a noise which could have some relevance to modeling g-jitter is the so-called Poissonian white shot noise, defined as a superposition of random instantaneous pulses, Poisson distributed in time, and with an amplitude that is exponentially distributed.

1. First passage time statistics for white noise

A complementary approach to study the dynamics of unstable stochastic systems is the so-called First Passage Time statistics.[27] In this approach, a random variable $t(x,x_0)$ is defined as the time needed to reach for the first time a prescribed value x given the initial condition $x(t=0)=x_0$. The stochastic process $x(t)$ is then characterized in terms of the statistics of $t(x,x_0)$.

For first-order and single variable stochastic equations with Gaussian white noise, the moments of the first passage time distribution $F(t)$ can be exactly reduced to quadrature.[27] Equation (7) is of second order in time but a first-order and single variable formulation can be defined within the so-called energy envelope approximation,[31] which exploits the separation of time scales between the variable $x(t)$ and the much slower variable $E(t)=\frac{1}{2}\dot{x}^2+\frac{1}{2}\omega_0^2x^2$. If the noise in Eq. (7) is Gaussian and white, then the probability distribution $P(E,t)$ obeys the Fokker–Planck equation,[28]

$$\frac{\partial}{\partial t}P(E,t)=\left[\frac{\partial}{\partial E}\left(\gamma-\frac{D}{\omega_0}\right)E+\frac{D}{2\omega_0^2}\frac{\partial^2}{\partial E^2}E^2\right]P(E,t), \tag{25}$$

which is equivalent to the stochastic equation for $E(t)$

$$\dot{E}=-\left(\gamma-\frac{D}{2\omega_0^2}\right)E+\frac{1}{\omega_0\sqrt{2}}E\xi(t), \tag{26}$$

where the noise satisfies $\langle\xi(t)\xi(t')\rangle=2D\delta(t-t')$. The mean first passage time $T(E,E_0)=\langle t(E,E_0)\rangle$ can be exactly calculated from the adjoint Fokker–Planck equation[27] associated to Eq. (25). With reflecting boundary at $E_r\to0$ and absorbing boundary at E_0 (Ref. 27) we find for $D-2\gamma\omega_0^2>0$,

$$T(E,E_0)=\frac{1}{(D/2\omega_0^2)-\gamma}\log\frac{E}{E_0}, \tag{27}$$

and for $D-2\gamma\omega_0^2<0$, $T(E,E_0)$ diverges.

If we average Eq. (26) we reproduce the result given in Eq. (24) taking into account that $\langle E\xi/\omega_0\sqrt{2}\rangle=D\langle E\rangle/2\omega_0^2$.[32] Interestingly, there is a gap $\gamma\omega_0^2<D<2\gamma\omega_0^2$ in which the system is energetically unstable (second moments diverging exponentially in time), but has a divergent mean first passage time. This can be interpreted as follows. For $D>2\gamma\omega_0^2$, the system is deterministically unstable according to Eq. (26), and on average, the time necessary to reach any value $E>E_0$ coincides exactly with that given by a purely deterministic evolution (with no noise). Below the deterministic threshold of Eq. (26), $D<2\gamma\omega_0^2$, the deterministic and noise terms have opposite effects. The former attracts trajectories $E(t)$ to the region near $E=0$, whereas the noise term has a destabilizing effect. The gap $\gamma\omega_0^2<D<2\gamma\omega_0^2$ corresponds to a situation in which, although the system is deterministically stable, a large enough number of realizations in the ensemble are driven by the noise term to large values of E. Since the effect of the noise is amplified by E, these trajectories will contribute considerably to the average $\langle E\rangle$ which then grows exponentially. The mean first passage time may still diverge because of the long time many trajectories are trapped in a neighborhood of $E=0$, where the dynamics is essentially deterministic and therefore stable. Finally, below the energetic instability threshold, enough realizations

are confined to small energies so that not only the mean first passage time diverges, but the mean energy decays.

This analysis illustrates the fact that when the noise spectrum is broad the response of the system has a rich statistics involving many time scales. In particular the first passage time distribution $F(t)$ has an algebraic decay at long times $F(t)\sim t^{-\delta}$ with $\delta=2-\gamma+(D/2\omega_0^2)$. The origin of this power law is the slowing down of the dynamics in the region of small energies, since in that region, both the stochastic and deterministic terms in Eq. (26) are very small.

The situation could be qualitatively different if other noise sources which may enter Eq. (26) or (7) additively, are considered. Such an additive noise (which is also desirable from a mathematical point of view to assure, for instance, the existence of a well-defined steady state[28]) is negligible in front of the multiplicative one except at $E\simeq 0$, where it dominates. Thus it could modify the asymptotic long time behavior of the first passage time distribution. However, since additive noise sources are not expected to modify the stability properties of $\langle E\rangle$,[28] they will not be considered here (see also Ref. 24).

In summary, we conclude that for noises of broad spectrum (close to white) the response of the parametric oscillator contains a wide range of time scales. Although a stability analysis based on second moments provides a useful criterion, it leads to a single time scale for instability, and therefore does not reproduce the rich statistics of the process. In particular, for a parameter range slightly above the energetic instability threshold, the average energy may grow exponentially, as a result of large contributions of relatively rare events, whereas a large number of trajectories may remain confined to small energies for relatively long times. On the other hand, even when the system is energetically stable and a steady state is well defined, higher-order moments may diverge as the energy distribution $P(E)$ develops a power-law decay at large energies, in contrast to the exponential decay when only additive noise sources are present.[28]

C. Narrow-band noise

In this section we will discuss different approximation schemes for the general case of narrow-band noise defined above as a Gaussian process with zero mean and autocorrelation,

$$\langle\xi(t)\xi(t')\rangle=\langle\xi^2\rangle e^{-|t-t'|/\tau}\cos\Omega(t-t'), \tag{28}$$

or a power spectrum,

$$P(\omega)=\frac{1}{2}\langle\xi^2\rangle\tau\left(\frac{1}{1+\tau^2(\Omega+\omega)^2}+\frac{1}{1+\tau^2(\Omega-\omega)^2}\right). \tag{29}$$

This process is characterized by three independent parameters, a characteristic frequency Ω, the characteristic width of the spectrum τ^{-1}, peaked at $\pm\Omega$, and the variance $\langle\xi^2\rangle$ equal to the area of the power spectrum. In the parameter range $\Omega\tau\gg 1$, the spectrum is very narrow and $\langle\xi^2\rangle$ is a useful measure of the the intensity of the noise. In the range close to white noise, $\Omega\tau\ll 1$, the spectrum is very broad and $\langle\xi^2\rangle$ diverges as τ^{-1}. In that case an appropriate measure of intensity of the noise is $D=\langle\xi^2\rangle\tau$, that is, the amplitude of the power spectrum rather than its area.

1. Low-frequency approximation for narrow-band noise

For narrow-band noise, it is possible to close the evolution equations for the statistical moments to lowest order in $\epsilon^2=(\omega_0^2+\gamma^2)/\Omega^2\ll 1$, that is, when the natural frequency of the oscillator is much smaller than the frequency of the driving term. This approximation entails expanding $x(t)$ around a slowly varying deterministic trajectory $\hat{x}(t)$. The general procedure is discussed in detail in Refs. 33 and 34. We use it here to study the stability of the set of equations (20) for finite values of τ and Ω. The method can be summarized as follows. Consider again the array $u(t)$, introduced in Eq. (18). Assume that each component u_i obeys an equation of the form

$$\dot{u}_i+\phi_i(u)=U_i[u,\xi(t)], \tag{30}$$

where $\xi(t)$ is a narrow-band noise. The stochastic trajectories $u_i(t)$ are expanded around a set of deterministic trajectories $\hat{u}_i(t)$ defined as the solution of Eq. (30) with $U_i\equiv 0$. In our case, $\partial\phi_i/\partial u_j\propto\mathcal{O}(\omega_0,\gamma)$, hence $\langle(\partial\phi_i/\partial u_j)[u_j(t)-\hat{u}_j(t)]\rangle$ can be neglected compared to $\langle U_i(u,t)\rangle$, and we can then write

$$\langle\dot{u}_i\rangle+\langle\phi_i\rangle=\left\langle\left(\frac{\partial U_i}{\partial u_k}\right)_{u=\hat{u}(t)}\int_0^t ds\, U_k[u(s),s]\right\rangle, \tag{31}$$

where summation over the index k is implied. We have also used the fact that $\langle U_i[\hat{u}(t),t]\rangle=0$. Equation (31) can be transformed by using mathematical identities (see Refs. 33 and 34) into

$$\begin{aligned}\langle\dot{u}_i\rangle+\langle\phi_i(x)\rangle&=\int_0^t ds\left\langle\left(\frac{\partial U_i}{\partial u_k}\right)_{u=u(t)}U_k[u(t),s]\right\rangle\\&\quad-\int_0^t ds\int_0^s ds'\left\langle\left(\frac{\partial U_i}{\partial u_k}\right)_{u=u(t)}\frac{d}{dt}U_k[u(t),s']\right\rangle,\end{aligned} \tag{32}$$

where we have also substituted $\hat{u}(t)$ by $u(t)$ and $(d/ds)\,U_k[u(s),s']$ by $(d/dt)\,U_k[u(t),s']$. If we now assume that the functions $U_i[u,\xi(t)]$ are of the form $U_i=v_i(u)\xi(t)$, Eq. (32) reduces to

$$\begin{aligned}\langle\dot{u}_i\rangle+\langle\phi_i(u)\rangle&=\frac{\tau}{1+(\Omega\tau)^2}\langle\xi^2\rangle\left\langle\frac{\partial v_i(u)}{\partial u_k}v_k(u)\right\rangle\\&\quad-\frac{\tau^2[1-(\Omega\tau)^2]}{[1+(\Omega\tau)^2]^2}\langle\xi^2\rangle\\&\quad\times\left\langle\frac{\partial v_i(u)}{\partial u_k}\frac{\partial v_k(u)}{\partial u_j}\dot{u}_j\right\rangle,\end{aligned} \tag{33}$$

where[33,34] the u dependence and the ξ dependence have been decoupled,

$$\langle F(u)\xi(t)\xi(s)\rangle \simeq \langle F(u)\rangle\langle\xi(t)\xi(s)\rangle, \tag{34}$$

the terms proportional to $\langle F(x)\rangle$ have been taken outside the integrals, and the upper limit of integration t has been replaced by ∞. In the case of the system of equations (20) (with the definitions $u_1=\omega_0^2x^2$, $u_2=\omega_0 x\dot{x}$ and $u_3=\dot{x}^2$) Eq. (33) reduces to

$$\begin{pmatrix}\langle\dot{u}_1\rangle\\ \langle\dot{u}_2\rangle\\ \langle\dot{u}_3\rangle\end{pmatrix}=\begin{pmatrix}0 & 2\omega_0 & 0\\ -\omega_0(1+B) & -\gamma & \omega_0\\ 2(A+\gamma B) & -2\omega_0 & -2\gamma\end{pmatrix}\begin{pmatrix}\langle u_1\rangle\\ \langle u_2\rangle\\ \langle u_3\rangle\end{pmatrix}, \tag{35}$$

where

$$A=\frac{\langle\xi^2\rangle}{\omega_0^2}\frac{\tau}{1+(\Omega\tau)^2},\quad B=2\frac{\langle\xi^2\rangle}{\omega_0^2}\frac{\tau^2[1-(\Omega\tau)^2]}{[1+(\Omega\tau)^2]^2}.$$

The prediction for the stability of the second moments in the low-frequency approximation is then given by the eigenvalue governing the stability of the system of equations (35) which reads

$$\lambda=-\gamma+\frac{\langle\xi^2\rangle\tau}{\omega_0^2}\frac{1}{1+(\Omega\tau)^2}. \tag{36}$$

Note that Eq. (36) reproduces the white noise result, Eq. (24) as $\tau\to 0$ with $\langle\xi^2\rangle\tau=D$ (finite).

2. Near resonance approximation for narrow-band noise

We have also been able to find an analytic approximation to the stability boundary of the parametric oscillator driven by narrow-band noise when $\omega_0\simeq\Omega/2$. We start by replacing the two independent variables x and $\dot{x}$ by z_1 and z_2 defined as follows:

$$x=z_1\cos\frac{\Omega t}{2}+z_2\sin\frac{\Omega t}{2},$$

$$\dot{x}=-\frac{\Omega z_1}{2}\sin\frac{\Omega t}{2}+\frac{\Omega z_2}{2}\cos\frac{\Omega t}{2},$$

where z_1 and z_2 will vary slowly in time compared to the sinusoidal component of frequency $\Omega/2$. Equation (7) may now be written as a pair of first-order equations for z_1 and z_2,

$$\begin{aligned}\Omega\dot{z}_1=&-\left[\frac{\Omega\gamma z_1}{2}+\left(\frac{\Omega^2}{4}-\omega_0^2\right)z_2\right]-\left[\left(\frac{\Omega^2}{4}-\omega_0^2\right)z_2\right.\\&\left.-\frac{\Omega\gamma z_2}{2}\right]\sin\Omega t+\xi(t)z_2\\&+\left[\frac{\Omega\gamma z_1}{2}+\left(\frac{\Omega^2}{4}-\omega_0^2\right)z_2\right]\cos\Omega t-\xi(t)\\&\times(-z_1\sin\Omega t+z_2\cos\Omega t),\end{aligned} \tag{37}$$

$$\begin{aligned}\Omega\dot{z}_2=&\left[\left(\frac{\Omega^2}{4}-\omega_0^2\right)z_1-\frac{\Omega\gamma z_2}{2}\right]+\left[\frac{\Omega\gamma z_1}{2}+\left(\frac{\Omega^2}{4}\right.\right.\\&\left.\left.-\omega_0^2\right)z_2\right]\sin\Omega t-\xi(t)z_1+\left[\left(\frac{\Omega^2}{4}-\omega_0^2\right)z_2\right.\\&\left.-\frac{\Omega\gamma z_2}{2}\right]\cos\Omega t-\xi(t)(z_1\cos\Omega t+z_2\sin\Omega t),\end{aligned} \tag{38}$$

where $\xi(t)$ is given by (8)–(10). By substituting Eq. (8) for $\xi(t)$ into Eqs. (37) and (38), we obtain

$$\begin{aligned}\Omega\dot{z}_1=&-\left[\frac{\Omega\gamma z_1}{2}+\left(\frac{\Omega^2}{4}-\omega_0^2\right)z_2\right]+\frac{1}{2}[S_2(t)z_1-S_1(t)z_2]\\&+\text{oscillatory terms},\end{aligned} \tag{39}$$

$$\begin{aligned}\Omega\dot{z}_2=&\left[\left(\frac{\Omega^2}{4}-\omega_0^2\right)z_1-\frac{\Omega\gamma z_2}{2}\right]-\frac{1}{2}[S_1(t)z_1+S_2(t)z_2]\\&+\text{oscillatory terms},\end{aligned} \tag{40}$$

where "oscillatory terms" stands for terms proportional to z_1 or z_2 with coefficients of the form $\sin\Omega t$, $\cos\Omega t$, $\sin 2\Omega t$, or $\cos 2\Omega t$. In the limit of $|(\Omega/2)-\omega_0|\ll\Omega$ (near the subharmonic parametric resonance) and $\gamma\ll\omega_0$ (the underdamped limit), we are interested in the slowly varying components z_1 and z_2 (compared to $\sin\Omega t$ and $\cos\Omega t$). When $\tau\gg 2\pi/\Omega$, the noise $S_1(t)$ or $S_2(t)$ also varies in a much slower time scale than $\sin\Omega t$ or $\cos\Omega t$. Hence the oscillatory terms may be neglected by averaging over a oscillating period while other terms remain. The statistics of the variables z_i can now be systematically computed by means of the cumulant expansion described in Sec. III B in the limit $|(\Omega/2)-\omega_0|\tau\ll 1$ and $(\gamma/2)\tau\ll 1$. Up to the second cumulant we find

$$\begin{aligned}\frac{d}{dt}\begin{pmatrix}\langle z_1^2\rangle\\ \langle z_1z_2\rangle\\ \langle z_2^2\rangle\end{pmatrix}&=\begin{pmatrix}-\gamma+3aP(2\beta) & -2\beta+2aQ(2\beta) & aP(2\beta)\\ \beta-aQ(2\beta) & -\gamma+2aP(2\beta) & -\beta+aQ(2\beta)\\ aP(2\beta) & 2\beta-2aQ(2\beta) & -\gamma+3aP(2\beta)\end{pmatrix}\\&\times\begin{pmatrix}\langle z_1^2\rangle\\ \langle z_1z_2\rangle\\ \langle z_2^2\rangle\end{pmatrix},\end{aligned} \tag{41}$$

where

$$a=\frac{\pi\langle\xi^2\rangle}{16\omega_0^2},\quad \beta=\frac{\Omega^2/4-\omega_0^2}{\Omega},$$

$$P(2\beta)=\frac{2\langle\xi^2\rangle}{\pi}\int_0^\infty e^{-t'/\tau}\cos(2\beta t')dt',$$

$$Q(2\beta)=\frac{2\langle\xi^2\rangle}{\pi}\int_0^\infty e^{-t'/\tau}\sin(2\beta t')dt'.$$

The stability of the second moments in the near resonance approximation, that is for $\pi|(\Omega/2)-\omega_0|/\omega_0 \ll |(\Omega/2)-\omega_0|\tau \ll 1$ and $\pi\gamma/\omega_0 \ll \gamma\tau \ll 1$, is then governed by the relevant eigenvalue of the matrix above, which reads

$$\lambda = -\gamma + \frac{\langle \xi^2 \rangle \tau}{2\omega_0^2} \frac{1}{1+(\Omega^2\tau^2/4)[1-(2\omega_0)^2/\Omega^2]^2}. \quad (42)$$

An approximate treatment when the spectrum is very narrow and centered exactly at resonance can be found in Ref. 31.

3. Neutral stability curve for arbitrary frequencies

In the general case of finite τ and Ω, and for arbitrary frequency ω_0, there is no systematic approximation scheme available. In this section we propose a nonsystematic approximation which reproduces the two controlled approximations we have described for low and near resonance frequencies (Secs. III C 1 and III C 2, respectively), and defines an extrapolation to the rest of the spectrum.

Assume that the underlying mechanism for instability in the stochastic case is still subharmonic parametric resonance. Furthermore, assume that stability is essentially determined by the amplitude of the power spectrum at $\omega = 2\omega_0$, which excites the dominant resonance. We can then use the result for white noise and replace the intensity of the white noise D by the corresponding value of the power spectrum of the narrow-band noise at the frequency $2\omega_0$. That is, we assume that the eigenvalue that determines the stability of the second-order moments, in the underdamped limit, is given by

$$\lambda = -\gamma + \frac{1}{\omega_0^2} P(2\omega_0). \quad (43)$$

Inserting the power spectrum Eq. (11) for narrow-band noise, Eq. (43) reads

$$\lambda = -\gamma + \frac{1}{2\omega_0^2}\langle \xi^2 \rangle \tau \left(\frac{1}{1+(\Omega\tau)^2(1-2\omega_0/\Omega)^2} + \frac{1}{1+(\Omega\tau)^2(1+2\omega_0/\Omega)^2} \right). \quad (44)$$

This is our central result. In principle, one would expect this ansatz to be valid for small enough τ, since, by construction, it is exact in the white noise limit. For Ornstein–Uhlenbeck noise ($\Omega=0$), it is exact within the cumulant expansion to second order, that is, to order D and all orders in τ,[30] since (44) reduces to (21), with $\langle \xi^2 \rangle = D/\tau$. For $\Omega \neq 0$, one can immediately check that the ansatz (44) also coincides with both results (36), for the low-frequency regime, and (42) for the near resonant region. Therefore the ansatz (44) reproduces the two controlled approximations discussed above in the range of parameters where they hold, interpolates smoothly between them in the intermediate frequency range, and defines an extrapolation to higher frequencies. Eventually, for large values of $\Omega\tau$, Eq. (44) is expected to fail. However, as we will show in the next section through numerical simulation of the stochastic harmonic oscillator, the neutral stability curve given by Eq. (44) is quantitatively accurate in the entire frequency spectrum for a large range of the parameter $\Omega\tau$.

IV. NUMERICAL SIMULATION OF THE STOCHASTIC PARAMETRIC OSCILLATOR

We have numerically simulated Eq. (7) with $\xi(t)$ the narrow-band random process defined in Eqs. (8) and (9), including the particular case of $\Omega=0$ [$\xi(t)$ is then an Ornstein–Uhlenbeck process]. An explicit second-order algorithm[35,36] was implemented in our simulation. We first rewrite Eq. (7) as

$$\dot{x} = y,$$

$$\dot{y} = -\gamma y - [\omega_0^2 + \xi(t)]x.$$

By expanding $x(t)$ and $y(t)$ in power series of time, and keeping up to order $\mathcal{O}(\Delta t^2)$, the following discretized equations result:

$$x(t+\Delta t) = x(t) + \Delta t y(t) - \tfrac{1}{2}\Delta t^2[\gamma y + \omega_0^2 x(t)] - x(t)\Gamma_2(t,\Delta t), \quad (45)$$

$$y(t+\Delta t) = y(t) - \Delta t[\gamma y(t) + \omega_0^2 x(t)] + \tfrac{1}{2}\Delta t^2[\gamma\omega_0^2 x(t) + \gamma^2 y(t) - \omega_0^2 y(t)] - [x(t) + \Delta t y(t)] \times \Gamma_1(t,\Delta t) + [\gamma x(t) + y(t)]\Gamma_2(t,\Delta t), \quad (46)$$

where

$$\Gamma_1(t,\Delta t) = \int_t^{t+\Delta t} dt'\, \xi(t'),$$

$$\Gamma_2(t,\Delta t) = \int_t^{t+\Delta t} dt' \int_t^{t'} dt''\, \xi(t''). \quad (47)$$

If $\xi(t)$ is an Ornstein–Uhlenbeck process with correlation time τ, such that $\langle \xi(t)\xi(t') \rangle = (D/\tau) \times \exp(-|t-t'|/\tau)$, it satisfies the equation

$$\frac{d\xi(t)}{dt} = -\frac{\xi(t)}{\tau} + \frac{\eta(t)}{\tau}, \quad (48)$$

where $\eta(t)$ is a Gaussian white noise with correlation, $\langle \eta(t)\eta(t') \rangle = 2D\delta(t-t')$. Equation (48) can be integrated to yield,

$$\xi(t+\Delta t) = e^{-\Delta t/\tau}\xi(t) + G_0(t,\Delta t), \quad (49)$$

with

$$G_0(t,\Delta t) = \frac{1}{\tau}\int_t^{t+\Delta t} dt' \exp\left(-\frac{t+\Delta t-t'}{\tau}\right)\eta(t').$$

By using Eq. (49), Γ_1 and Γ_2 can be written as,

$$\Gamma_1(t,\Delta t) = \tau(1-e^{-\Delta t/\tau})\xi(t) + G_1(t,\Delta t),$$

$$\Gamma_2(t,\Delta t) = \tau^2(\Delta t/\tau + e^{-\Delta t/\tau} - 1)\xi(t) + G_2(t,\Delta t),$$

where G_1 and G_2 are also random variables. The variances and cross-correlations of Γ_1 and Γ_2 can now be calculated from the variances and cross-correlations of $\xi(t)$, G_1, and G_2. The quantities G_0, G_1, and G_2 are not independent and

can be obtained from two independent Gaussian random numbers with zero mean and unit variance.[36] Furthermore, $\langle G_2^2 \rangle$ is $\mathcal{O}(\Delta t^5)$ and can be neglected. Given $x(t)$, $y(t)$, and $\xi(t)$, integration proceeds as follows. Two independent random numbers with zero mean and unit variance are generated and used to obtain G_0, G_1, and G_2, with the appropriate factors (function of Δt), to ensure that these latter variables are distributed with the correct variance. Equations (50) are then used to find Γ_1 and Γ_2, which inserted into Eqs. (45) and (46) yield $x(t+\Delta t)$ and $y(t+\Delta t)$. Equation (48) is used to obtain $\xi(t+\Delta t)$.

We have developed a similar algorithm for the case of narrow-band noise. The equations for the oscillator, discretized in the same manner and keeping the changes in $x(t)$ and $y(t)$ up to order $\mathcal{O}(\Delta t^2)$, are again Eqs. (45) and (46). The noise $\xi(t)$ is now given by Eqs. (8), (9), and (10). Since S_1 and S_2 in those equations are themselves Ornstein–Uhlenbeck processes, they each satisfy

$$S_1(t+\Delta t) = e^{-\Delta t/\tau} S_1(t) + F_0(t,\Delta t),$$

$$S_2(t+\Delta t) = e^{-\Delta t/\tau} S_2(t) + H_0(t,\Delta t),$$

where

$$F_0(t,\Delta t) = \frac{1}{\tau} \int_t^{t+\Delta t} dt' \exp\left(-\frac{t+\Delta t-t'}{\tau}\right) \eta_1(t'),$$

$$H_0(t,\Delta t) = \frac{1}{\tau} \int_t^{t+\Delta t} dt' \exp\left(-\frac{t+\Delta t-t'}{\tau}\right) \eta_2(t'),$$

and $\eta_1(t)$ and $\eta_2(t)$ are two independent Gaussian white noises: $\langle \eta_1(t)\eta_1(t') \rangle = \langle \eta_2(t)\eta_2(t') \rangle = 2D\delta(t-t')$. In Eqs. (45) and (46) Γ_1 and Γ_2 can now be written as

$$\Gamma_1(t,\Delta t) = \frac{\tau}{1+\Omega^2\tau^2} (\{\cos \Omega t - \Omega\tau \sin \Omega t - e^{-\Delta t/\tau}[\cos \Omega(t+\Delta t) - \Omega\tau \sin \Omega(t+\Delta t)]\} S_1(t) + \{\sin \Omega t + \Omega\tau \cos \Omega t$$
$$- e^{-\Delta t/\tau}[\sin \Omega(t+\Delta t) + \Omega\tau \cos \Omega(t+\Delta t)]\} S_2(t)) + F_1(t,\Delta t) + H_1(t,\Delta t), \tag{50}$$

$$\Gamma_2(t,\Delta t) = \frac{\tau^2}{1+\Omega^2\tau^2} \left[\left(\frac{1-\Omega^2\tau^2}{1+\Omega^2\tau^2} [e^{-\Delta t/\tau} \cos \Omega(t+\Delta t) - \cos \Omega t] - \frac{2\Omega\tau}{1+\Omega^2\tau^2} [e^{-\Delta t/\tau} \sin \Omega(t+\Delta t) - \sin \Omega t] \right.\right.$$
$$\left. + \frac{\Delta t}{\tau} (\cos \Omega t - \Omega\tau \sin \Omega t) \right) S_1(t) + \left(\frac{1-\Omega^2\tau^2}{1+\Omega^2\tau^2} [e^{-\Delta t/\tau} \sin \Omega(t+\Delta t) - \sin \Omega t] - \frac{2\Omega\tau}{1+\Omega^2\tau^2} \right.$$
$$\left.\left. \times [e^{-\Delta t/\tau} \cos \Omega(t+\Delta t) - \cos \Omega t] + \frac{\Delta t}{\tau} (\sin \Omega t + \Omega\tau \cos \Omega t) \right) S_2(t) \right] + F_2(t,\Delta t) + H_2(t,\Delta t). \tag{51}$$

Expressions for F_1, H_1, F_2, and H_2, their variances and cross-correlations are listed in the Appendix. In order to obtain them, four independent Gaussian random numbers with zero mean and unit variance, r_1, r_2, r_3, and r_4 are needed, $F_0 = Ar_1$, $F_1 = Br_1 + Cr_2$, $F_2 = Dr_1 + Er_2$, where A, B, C, D, and E can be readily calculated from $\langle F_0^2 \rangle$, $\langle F_1^2 \rangle$, $\langle F_0 F_1 \rangle$, $\langle F_0 F_2 \rangle$, and $\langle F_1 F_2 \rangle$. Similarly H_0, H_1, and H_2 can be obtained from another two Gaussian random numbers, r_3 and r_4.

Here we shortly summarize the simulation algorithm. First, once Δt has been fixed, variances and cross-correlations for the F_i and H_i can be computed. Initial conditions $x(t=0)$ and $y(t=0)$ are chosen to be two independent Gaussian random numbers, with zero mean and unit variance. Four independent Gaussian random numbers with zero mean and unit variance are generated, and used to obtain F_i and H_i. They are then inserted into Eqs. (50) and (51) to obtain Γ_1 and Γ_2. Equations (45) and (46) are then used to determine $x(\Delta t)$ and $y(\Delta t)$. The equations are integrated up to a time $t_{\max}$ that depends on ω_0, γ, and the parameters of the noise. With $\gamma = 0.005$, or 0.008, a typical value of $t_{\max}$ is $t_{\max} = 100\pi/\omega_0$, although for simulations with large $\tau > 5$, integrations were conducted up to $t_{\max} \sim 200\pi/\omega_0 - 300\pi/\omega_0$, and for small $\omega_0 \lesssim 0.1$, $t_{\max} \sim 20\pi/\omega_0 - 50\pi/\omega_0$. To obtain the statistical moments of the system variables $x(t)$ and $y(t)$, we repeat this procedure a sufficiently large number of times N. Typically $N = 5000$. For the case of an Ornstein–Uhlenbeck process, the simulations were done for $\omega_0 = 1.0$, $\gamma = 0.005$, $\tau = 0.1$, 0.5, 1.0, 2.0, 3.0, 4.0, 5.0, and several values of the noise intensity D both below and above the critical D_c for instability of the second moments. The second-order algorithm developed allows one to use relatively large time steps. A time step of $\Delta t = 0.1$ was used for all the values of τ. We compared the simulation results obtained by setting $\Delta t = 0.1$ to those obtained by choosing a smaller time step, $\Delta t = 0.01$. A very good agreement was found even for the smallest τ used ($\tau = 0.1$). We note that the particular value of $\Delta t = 0.1$ is essentially determined by the deterministic part of Eq. (7), and that, of course, $\tau \geqslant \Delta t$. For the case of a narrow-band noise, numerical simulations of Eq. (7) were done for fixed values of $\Omega = 2.0$, $\gamma = 0.008$, but different values of ω_0 ranging from $\omega_0 = 0.04$ to 2.0 to study the resonant behavior, and $\tau = 0.1$, 0.5, 1.0, 3.0, 5.0, 10.0, 15.0; Δt was set to 0.05 or 0.1.

The analysis of the simulation results focused on the second moment of x, $\langle x^2 \rangle$. In the underdamped limit, analytical results when $\xi(t)$ is an Ornstein–Uhlenbeck process or a narrow-band noise, both far from resonance and near resonance, predict one real and two complex conju-

gate eigenvalues for the linear evolution equation of the second moments $\langle x^2\rangle$, $\langle \dot{x}x\rangle$, and $\langle \dot{x}^2\rangle$, where the real eigenvalue is relevant to the energetic stability of the system. This is expected to be approximately true for a general narrow-band noise as well. Thus we have

$$\langle x^2\rangle = a_0 \exp(\lambda t) + a_1 \exp(\lambda' t)\cos(2\omega_0' t + \phi_0), \quad (52)$$

where a_0, a_1, λ, λ', ω_0', and ϕ_0 are all real constants. To obtain the relevant eigenvalue λ, we fit the $\langle x^2\rangle$ data to a simple exponential function $a_0 \exp(\lambda t)$ since, in the underdamped limit ($\gamma^2/4\omega_0^2 \ll 1$), the oscillating part of (52) is averaged out by the fitting procedure. In our simulations for the Ornstein–Uhlenbeck case, the ratio $\gamma^2/4\omega_0^2$ is of the order of 10^{-6}. For the narrow-band noise simulations, it ranges between 10^{-6} for large frequencies to 10^{-2} for low frequencies. In the latter case a single exponential fit is less accurate [the theoretical prediction also has corrections of order $\gamma^2/4\omega_0^2$ which have not been included in Eq. (44)]. The critical value of noise intensity D_c, defined by $\lambda(D_c)=0$ is obtained by interpolating the curve λ vs D obtained in both the stable and unstable regimes. It is worth mentioning that moments of fourth order may diverge in some cases, producing a statistical error on the second moments that grows exponentially in time. In none of the cases studied, however, has an ensemble of more than 10 000 realizations been necessary.

The numerical procedure was first checked against the exact result for white noise. In the limit of $\tau \to 0$, both the Ornstein–Uhlenbeck noise and the narrow-band noise with nonzero Ω become a Gaussian white noise. The critical value for instability D_c for the smallest correlation time used $\tau=0.1$ differs by less than 1% from the exact result for Gaussian white noise when $\xi(t)$ is an Ornstein–Uhlenbeck process, and less than 10% when $\xi(t)$ is a narrow-band noise with ω_0/Ω ranging from 0 to 1.

We have first studied the critical noise intensity D_c as a function of τ for Ornstein–Uhlenbeck noise ($\Omega=0$). The result is shown in Fig. 1, where it is compared with two analytical approximations based on different resummation schemes of the orders τ^n.[28,30] In this case, our ansatz (44) coincides exactly with the prediction of Ref. 30. An excellent agreement is found in the short correlation time regime ($\omega_0\tau \lesssim 1$). For larger correlation times, the theoretical predictions of the critical noise intensity is higher than the numerical results. This figure shows that the effect of decreasing the width of the spectrum while keeping its maximum value D constant (at $\omega=0$) is to enhance stability. This fact can be interpreted as a consequence of the reduction in the amplitude of the power spectrum at the frequency $2\omega_0$ which excites the parametric resonance.

We next discuss our results for narrow-band noise. We wish to test the validity of the far from resonance approximation, the near resonance approximation, and the ansatz proposed in the previous section as the parameters of the noise are varied. Figure 2(a) shows the simulation results for the stability boundaries of $\langle x^2\rangle$ for $\Omega\tau=0.2$, 1.0, 2.0, 6.0, and a wide range of frequencies. The agreement is very good in the entire frequency range investigated. This suggests that the underlying physical assumption about the dominant role of the subharmonic resonance for narrow-band noise is essentially correct. Simulation results for larger $\Omega\tau$ are shown in Fig. 2(b). For $\Omega\tau$ as large as ~ 30, the prediction of the ansatz still agrees with numerical results reasonably well. Further comparison between the simulation results and the prediction of the ansatz exactly at the subharmonic resonance $\omega_0/\Omega=0.5$ is shown in Fig. 3. The prediction of the ansatz agrees very well with the numerical result for small $\Omega\tau$. The deviation is about 10% below the simulation result for $\Omega\tau \sim 30$.

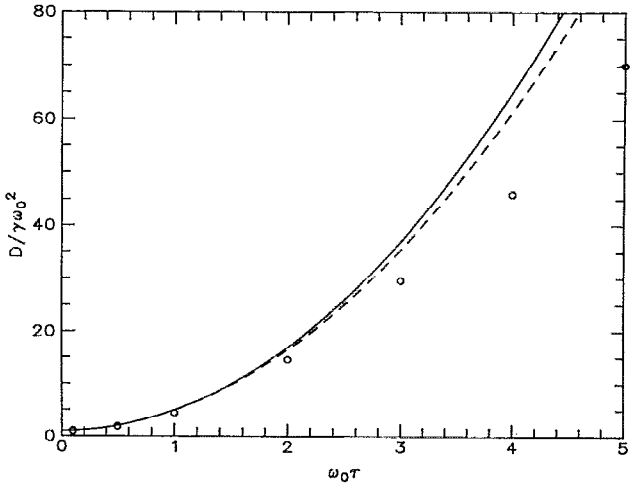

FIG. 1. Stability boundaries for the second moments of the parametric harmonic oscillator driven by Ornstein–Uhlenbeck noise. Instability occurs above the lines shown. The figure shows the dimensionless noise intensity $D/\gamma\omega_0^2$, where ω_0 is the natural frequency of the oscillator and γ the friction coefficient, versus the dimensionless correlation time $\omega_0\tau$. The solid line is the perturbative result obtained by van Kampen,[30] which is valid to first order in D and all orders in τ. The dashed line is the approximate result given by Lindenberg and West.[28] The circles are the results of our numerical simulations.

V. APPLICATION TO TYPICAL MICROGRAVITY CONDITIONS

Although a precise characterization of residual accelerations in a microgravity environment is under way, there is enough information already available for our purposes. The spectral density of g-jitter determined during various space missions does have one or several dominant frequencies, but it is also quite broad. We consider spectral densities like the ones shown in Refs. 13 and 15. The dominant frequencies are in the range 1–20 Hz, hence Ω is in the range $2\pi(1\text{–}20)\,\text{sec}^{-1}$. Characteristic widths of the spectral density are 5–10 Hz, or τ between 0.1–0.2 sec; therefore $\Omega\tau \sim 1\text{–}25$. An important aspect that remains open due to the lack of data is the Gaussian or non-Gaussian character of the actual g-jitter. As noted above, this could lead to quantitatively different results, and therefore it would be interesting to have this kind of information available.

We next determine the value of $\langle \xi^2\rangle$. Note from Eqs. (6) and (7) that $\xi(t) = -q g_z(t)$, hence $\langle \xi^2\rangle = q^2\langle g_z^2\rangle$, with $\langle g_z^2\rangle$ being proportional to the area beneath the spectral density of g-jitter measured. From Fig. 9 in Ref. 13 (which

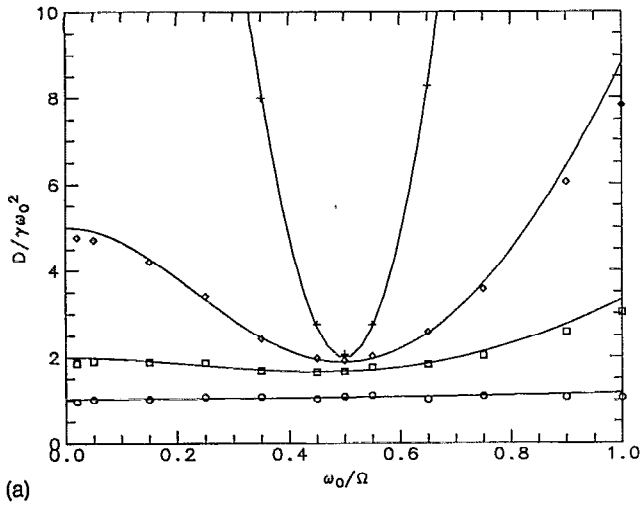

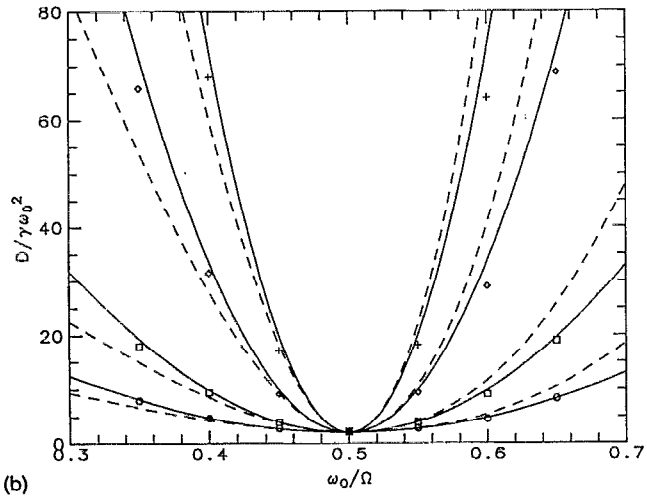

FIG. 2. Stability boundaries for the second moments of the parametric harmonic oscillator driven by narrow-band noise. The figure shows the dimensionless noise intensity $D/\gamma\omega_0^2$ vs ω_0/Ω, where ω_0 is the natural frequency of the oscillator and Ω the characteristic frequency of the noise. Several correlation times are shown: (a) ○, $\Omega\tau=0.2$; □, $\Omega\tau=1.0$; ◇, $\Omega\tau=2.0$; and ×, $\Omega\tau=6.0$. The solid line is the ansatz given in Eq. (44). (b) Same as in (a), but larger correlation times are shown, ○, $\Omega\tau=6.0$; □, $\Omega\tau=10.0$; ◇, $\Omega\tau=20.0$; and ×, $\Omega\tau=30.0$. The solid line is the ansatz given in Eq. (44), and the dashed line is the near resonance approximation given in Eq. (42).

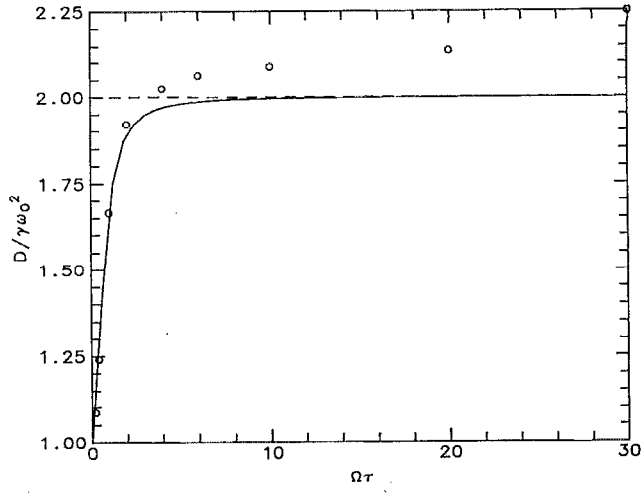

FIG. 3. Critical value for instability of the second moments of the parametric harmonic oscillator driven by narrow-band noise at resonance, $\Omega=2\omega_0$, versus dimensionless correlation time $\Omega\tau$. Here ω_0 is the natural frequency of the oscillator and Ω is the characteristic frequency of the noise. The circles are the results of the numerical simulations, the solid line the ansatz given in Eq. (44), and the dashed line, the near resonance approximation given in Eq. (42). As it is discussed in the text, the ansatz becomes exact in the limit of white noise ($\tau\to 0$). For the largest value of $\Omega\tau$ studied, the difference between Eq. (44) and our numerical calculations in around 10%.

gives the power spectral density of a representative time window aboard Spacelab 3), we estimate $G=\sqrt{\langle g_j^2\rangle}\approx 8\times 10^{-4} g_E$. This is a very conservative estimate; considerably larger values can be obtained from this and other published measurements (see, e.g., Figs. 1 and 2 in Ref. 15).

Contact with the results obtained for the parametric oscillator can be made by replacing $\gamma=4\nu q^2$, $\omega_0^2\approx(\Gamma/\rho)q^3$ and $\xi(t)=-qg_z(t)$. Note that γ and ω_0 are no longer independent from each other, implying that in the limit $q\to 0$ the system is actually approaching the underdamped limit, since $\gamma^2/4\omega_0^2=4\nu^2\rho\Gamma^{-1}q$. The stability boundary predicted by Eq. (44) can now be written as

$$\frac{G^2}{\nu\Omega^3}=4\frac{\omega_0^2}{\Omega^2}\frac{1+2(\Omega\tau)^2[1+4(\omega_0/\Omega)^2]+(\Omega\tau)^4[1-4(\omega_0/\Omega)^2]^2}{\Omega\tau\{1+(\Omega\tau)^2[1+4(\omega_0/\Omega)^2]\}}. \tag{53}$$

Equation (53) is plotted in Fig. 4(a) for several representative values of $\Omega\tau$. The points above the curves correspond to the unstable region. For small values of $\Omega\tau$, the stability boundary increases monotonically with ω_0/Ω. At approximately $(\Omega\tau)_c\approx 1.555$, an additional minimum appears. As $\Omega\tau$ is further increased, the dimensionless frequency of the new minimum approaches 0.5 from the left, and the value of $G^2/\nu\Omega^3$ at the minimum continuously decreases, approaching zero as $\Omega\tau\to\infty$. For arbitrarily small values of G, there is always a band of unstable frequencies in the vicinity of $\omega_0/\Omega=0$. This fact reflects the effective enhancement of the noise at low frequencies by the factor $1/\omega_0^2$ in the last term of Eq. (44). For $\Omega\tau>(\Omega\tau)_c$, and fixed $G^2/\nu\Omega^3$, it is possible to have two bands of unstable solutions: one at small frequencies, the other around the region of subharmonic resonance.

For the parameter ranges estimated for typical g-jitter, the low-frequency instability is likely to be unobservable

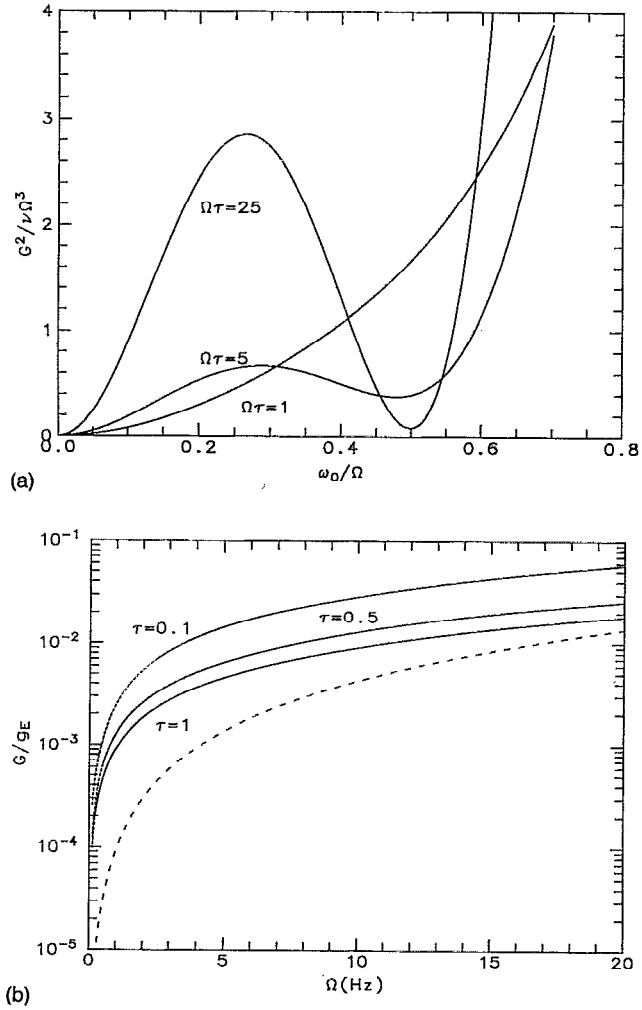

FIG. 4. (a) Stability boundaries for the second moments of free surface away from planarity. The figure shows the dimensionless mean-squared fluctuations in gravitational acceleration versus the dimensionless frequency of the surface modes. The intensity of the fluctuations in the gravitational field is given by $G^2=\langle g_z(t)^2\rangle$, ν is the kinematic viscosity of the fluid, Ω the characteristic frequency of the narrow-band noise, and ω_0 the frequency of the surface mode. Different curves show the stability boundaries for various values of the dimensionless correlation time $\Omega\tau$. We note that for $\Omega\tau\geqslant 1.555$, the neutral stability curve has one minimum at a finite value of ω_0/Ω. Below that value, the only minimum is at $\omega_0/\Omega=0$. (b) Estimate of tolerable levels of g-jitter for instability of a planar water–air surface at room temperature. We show the normalized root-mean-squared g-jitter for instability as a function of the characteristic frequency of the driving noise (g_E is the intensity of the gravitational field on the Earth's surface). Three different correlation times are shown, as indicated in the figure. The solid lines refer to those regions of $\Omega\tau$ for which the stability curve has a minimum at finite frequencies [see (a)]. The dotted lines correspond to the stability boundary of (a) at $\omega_0=\Omega/2$, in the region where that curve does not have a minimum. The dashed line is the stability curve for the Mathieu equation for the same driving frequency.

because it may correspond to wavelengths larger than the natural long wavelength cutoff defined by the container size. For instance, for fluid parameters appropriate to a water–air surface at room temperature $\nu=0.01$ cm^2/sec, $\Gamma=75.5$ ergs/cm^2, and $\rho=1$ g/cm^3, with $\Omega\sim 12$ Hz and $G\sim 10^{-3}\ g_E$, the shortest wavelength of the long wavelength band ranges from 15 to 35 cm for $\Omega\tau$ in the range 1–25.

Given that the low-frequency band is not likely to be observable, the absolute threshold for instability will typically be given by the minimum of Eq. (53). In Fig. 4(b) we have plotted the threshold given by Eq. (53) at $\omega=\Omega/2$, as a function of Ω for several values of τ. [The minimum of Eq. (53) is not exactly at $\omega=\Omega/2$, but the values of $G^2/\nu\Omega^3$ at the exact minimum and at $\omega=\Omega/2$ do not differ significantly.] The dashed portion of the curve corresponds to the region where there is no resonance minimum. For comparison purposes, we have also plotted the stability boundary of the deterministic case given by, $\xi(t)=\xi_0\cos(\Omega t)$. The threshold for instability for this case is known.[25] For subharmonic resonance, instability occurs if

$$\left(\frac{\xi_0}{2\omega_0}\right)^2-\gamma^2\geqslant 0. \tag{54}$$

As it has been already discussed in Sec. III, in order to compare this case with the results of our previous calculation, we have $\langle\xi^2\rangle=\xi_0^2/2$, i.e., $q^2\langle g_z^2\rangle=\xi_0^2/2$. The threshold for instability of the resonant mode with $\omega_0=\Omega/2$ in this case is given by

$$(G_c)_{\text{det}}=\nu\sqrt{2}\left(\frac{2\rho\Omega^5}{\Gamma}\right)^{1/3}. \tag{55}$$

Finally Fig. 4(b) shows that the interface becomes effectively more stable as τ is decreased, at constant G (i.e., at constant area of the power spectrum). This has the clear interpretation that the forcing is less efficient in exciting the resonance as it spreads into a band of frequencies, as opposed to being concentrated at the resonant frequency. For the range of frequencies 5–20 Hz we see that a g-jitter level of $G\simeq 10^{-3}\ g_E$ lies below all curves and therefore it does not lead to instability for the case of a water–air surface at room temperature.

VI. SUMMARY AND CONCLUSIONS

We have studied the linear response of the free surface of an incompressible fluid subjected to a random effective gravity (or g-jitter) directed along the normal to the surface at rest. Each spatial Fourier component of the surface displacement satisfies the equation of the parametric harmonic oscillator. We have focused our attention, however, on the case in which the driving force is of random nature. A narrow-band stochastic process has been introduced as a model of g-jitter. The process is characterized by its intensity G^2, a characteristic frequency Ω, and a correlation time τ. This process interpolates smoothly between the limit of white noise ($\Omega\tau\to 0$), in which no frequency component is preferred, and the limit of monochromatic noise ($\Omega\tau\to\infty$), corresponding to a single frequency forcing while still containing a distribution of amplitudes and phases.

Stability of the solutions of the parametric oscillator has been defined with respect to the second-order statistical moments of the oscillator coordinate because of their rela-

tion to the energy of the oscillations. The neutral stability curve has been obtained analytically in the limit of low frequencies, and close to the subharmonic instability. An interpolation formula with no adjustable parameters has been derived that reduces to the two asymptotic forms in the two limits discussed. The main assumption underlying the interpolation formula is that even in the stochastic case the dominant response of a surface mode of natural frequency ω_0 is subharmonic resonance, and is determined by the intensity of the driving noise at $2\omega_0$. The approximation is seen to break down in the limit $\Omega\tau \gg 1$, but is found to be numerically accurate up to $\Omega\tau \sim 30$. The values of $\Omega\tau$ estimated for g-jitter lie well within this range of validity.

The effects of varying the width of the noise spectrum on the stability of the parametric oscillator can be summarized as follows. In the region close to white noise ($\tau \simeq 0$), the noise intensity is determined by the parameter $D = \langle \xi^2 \rangle \tau$. The effect of increasing the correlation time τ while keeping D constant is in the direction of increasing stability. This had been predicted by approximate theories for the case of Ornstein–Uhlenbeck noise ($\Omega = 0$),[28] and has been explicitly checked numerically. The same general conclusion is found to apply for $\Omega \neq 0$. We interpret this result to be a consequence of decreasing the intensity of the power spectrum at the corresponding subharmonic resonant frequency. In the opposite limit, $\Omega\tau \gg 1$, the strength of the external driving force is given $\langle \xi^2 \rangle$, which is proportional to the area beneath the power spectrum. In this case, the broadening of the spectrum (decreasing τ) at constant $\langle \xi^2 \rangle$ has a stabilizing effect on the frequency at subharmonic resonance. This is interpreted as a lack of efficiency in exciting the resonance when the noise effectively spans a larger range of frequencies and cannot persist at resonance for very long times. The same trends would apply to a system which only has a discrete set of natural frequencies.

We have developed a numerical algorithm, of second order with respect to the integration variables and exact in the stochastic contribution, to solve the equation of the parametric harmonic oscillator driven by narrow-band noise. Excellent agreement between the numerical and analytical results has been found for the entire range of parameters investigated. The extension of the algorithm to spatially extended systems is straightforward and is currently being implemented for the system of partial differential equations that describe fluid motion.

Two main conclusions emerge from our study. First, an external driving force with a broad frequency spectrum leads to parametric resonance in a wide frequency range. The resonant behavior is not given by the superposition of the resonances produced by each of the frequency components because of the nonlinear coupling between the external force and the oscillator coordinate. Second, the resonant behavior of the second moments (or the energy) is in general weaker than the resonance that would result from any of the frequency components acting alone, at equal area of the power spectrum.

We conclude by pointing out that our findings for the stochastic parametric oscillator driven by narrow-band noise can be straightforwardly applied to other cases in which the underlying mode of instability satisfies the equation of the parametric oscillator, such as the stress-free Rayleigh–Bénard problem, or thermosolutal convection during directional solidification. Furthermore, there are situations, e.g., a diffusion couple, in which the restoring force of surface tension is absent, and the effects of g-jitter are expected to be more pronounced. The analysis of these cases is deferred to future work.

ACKNOWLEDGMENTS

We are indebted to Bob Sekerka for many stimulating discussions and a careful reading of the manuscript. We also thank Vlad Shapiro for many interesting discussions.

This work is supported by the Microgravity Science and Applications Division of NASA under Contract No. NAG3-1284. This work is also supported in part by the Supercomputer Computations Research Institute, which is partially funded by the U.S. Department of Energy, Contract No. DE-FC05-85ER25000.

APPENDIX: EXPRESSIONS FOR F_1, F_2, AND THEIR CORRELATIONS

Here we list the expressions and variances of F_1 and F_2, and the cross-correlations $\langle F_0 F_1 \rangle$, $\langle F_0 F_2 \rangle$, and $\langle F_1 F_2 \rangle$. Similar quantities for H_i can be obtained from the corresponding terms for F_i by replacing $\cos \Omega t \to \sin \Omega t$ and $\sin \Omega t \to -\cos \Omega t$:

$$F_1(t,\Delta t) = -\frac{1}{1+\Omega^2\tau^2} \int_t^{t+\Delta t} dt' \left[[\cos \Omega(t+\Delta t) - \Omega\tau \sin \Omega(t+\Delta t)] \exp\left(-\frac{t+\Delta t-t'}{\tau} \right) \right.$$

$$\left. -\cos \Omega t' + \Omega\tau \sin \Omega t' \right] \eta_1(t'),$$

$$F_2(t,\Delta t)=\frac{-1}{1+\Omega^2\tau^2}\left\{\frac{2\Omega\tau^2}{1+\Omega^2\tau^2}\int_t^{t+\Delta t}dt'\left[\sin\Omega(t+\Delta t)\exp\left(-\frac{t+\Delta t-t'}{\tau}\right)-\sin\Omega t'\right]\eta_1(t')\right.$$
$$-\frac{1-\Omega^2\tau^2}{1+\Omega^2\tau^2}\int_t^{t+\Delta t}dt'\left[\cos\Omega(t+\Delta t)\exp\left(-\frac{t+\Delta t-t'}{\tau}\right)-\cos\Omega t'\right]\eta_1(t')$$
$$\left.-\int_t^{t+\Delta t}dt'(t+\Delta t-t')(\cos\Omega t'-\Omega\tau\sin\Omega t')\eta_1(t')\right\}.$$

The variances and cross-correlation functions are

$$\langle F_1^2\rangle=\frac{2D}{(1+\Omega^2\tau^2)^2}\left(\frac{1+\Omega^2\tau^2}{2}\Delta t+\frac{1-\Omega^2\tau^2}{4\Omega}[\sin 2\Omega(t+\Delta t)-\sin 2\Omega t]+\frac{\tau}{2}[\cos 2\Omega(t+\Delta t)-\cos 2\Omega t]\right.$$
$$+\frac{\tau}{2}(1-e^{-2\Delta t/\tau})[\cos\Omega(t+\Delta t)-\Omega\tau\sin\Omega(t+\Delta t)]^2-2\tau[\cos\Omega(t+\Delta t)-\Omega\tau\sin\Omega(t+\Delta t)]$$
$$\left.\times[\cos\Omega(t+\Delta t)-e^{-\Delta t/\tau}\cos\Omega t]\right),$$

$$\langle F_2^2\rangle=\frac{2D}{(1+\Omega^2\tau^2)^2}\left[\frac{\Delta t\tau}{2}(\tau-\Delta t)+\frac{\Delta t^3(1+\tau^2\Omega^2)}{6}+\frac{\tau^3}{4}(1-e^{-2\Delta t/\tau})\right.$$
$$\times\left(1+\frac{(1-6\tau^2\Omega^2+\tau^4\Omega^4)\cos 2\Omega(t+\Delta t)-2\tau\Omega(1-\tau^2\Omega^2)\sin 2\Omega(t+\Delta t)}{(1+\tau^2\Omega^2)^2}\right)+\frac{1}{4\Omega}\left(\frac{\tau^2(\Omega^4\tau^4-5\Omega^2\tau^2-2)}{(1+\Omega^2\tau^2)^2}\right.$$
$$\left.-\frac{1-\Omega^2\tau^2}{2\Omega^2}\right)[\sin 2\Omega(t+\Delta t)-\sin 2\Omega t]-\frac{2\Omega^2\tau^5}{(1+\Omega^2\tau^2)^2}[\cos 2\Omega(t+\Delta t)-\cos 2\Omega t]+\frac{\Delta t\tau}{2(1+\Omega^2\tau^2)}$$
$$\times\left(\tau(3-\Omega^2\tau^2)\cos 2\Omega t+\frac{1-3\Omega^2\tau^2}{2\Omega}\sin 2\Omega t\right)-\frac{2\tau^2}{(1+\Omega^2\tau^2)^2}[2\Omega\tau\sin\Omega(t+\Delta t)-(1-\Omega^2\tau^2)\cos\Omega(t+\Delta t)]$$
$$\left.\times\{2\Omega\tau^2\sin\Omega(t+\Delta t)-e^{-\Delta t/\tau}[2\Omega\tau^2\sin\Omega t+(1+\Omega^2\tau^2)\Delta t\cos\Omega t]\}\right],$$

$$\langle F_0F_1\rangle=\frac{2D}{1+\Omega^2\tau^2}\left([\cos\Omega(t+\Delta t)-e^{-\Delta t/\tau}\cos\Omega t]-\frac{1}{2}(1-e^{-2\Delta t/\tau})[\cos\Omega(t+\Delta t)-\Omega\tau\sin\Omega(t+\Delta t)]\right),$$

$$\langle F_0F_2\rangle=\frac{2D}{(1+\Omega^2\tau^2)^2}\left[(1-e^{-2\Delta t/\tau})\left(\frac{\tau(1-\Omega^2\tau^2)}{2}\cos\Omega(t+\Delta t)-\Omega\tau^2\sin\Omega(t+\Delta t)\right)+2\Omega\tau^2[\sin\Omega(t+\Delta t)\right.$$
$$\left.-e^{-\Delta t/\tau}\sin\Omega t]-\Delta te^{-\Delta t/\tau}\cos\Omega t\right],$$

$$\langle F_1F_2\rangle=\frac{2D}{(1+\Omega^2\tau^2)^2}\left[-\frac{\Delta t}{2}\left(\tau-\frac{\Delta t(1+\Omega^2\tau^2)}{2}\right)+\frac{\Omega\tau^3}{1+\Omega^2\tau^2}[\sin 2\Omega(t+\Delta t)-\sin 2\Omega t]+\frac{\tau^2}{1+\Omega^2\tau^2}[(1-\Omega^2\tau^2)\cos\Omega\right.$$
$$\times(t+\Delta t)-2\Omega\tau\sin\Omega(t+\Delta t)][\cos\Omega(t+\Delta t)-e^{-\Delta t/\tau}\cos\Omega t]-\frac{1+6\Omega^2\tau^2-3\Omega^4\tau^4}{8\Omega^2(1+\Omega^2\tau^2)}[\cos 2\Omega(t+\Delta t)$$
$$-\cos 2\Omega t]-\frac{\Delta t}{2}\left(\frac{1-\Omega^2\tau^2}{2\Omega}\sin 2\Omega t+\tau\cos 2\Omega t\right)+\frac{\tau^2(1-e^{-\Delta t/\tau})}{2(1+\Omega^2\tau^2)}[2\Omega\tau\sin\Omega(t+\Delta t)-(1-\Omega^2\tau^2)\cos\Omega$$
$$\times(t+\Delta t)][\cos\Omega(t+\Delta t)-\Omega\tau\sin\Omega(t+\Delta t)]-[\cos\Omega(t+\Delta t)-\Omega\tau\sin\Omega(t+\Delta t)]\frac{2\Omega\tau^3}{1+\Omega^2\tau^2}$$
$$\left.\times[\sin\Omega(t+\Delta t)-e^{-\Delta t/\tau}\sin\Omega t]-\Delta t\tau e^{-\Delta t/\tau}\cos\Omega t\right].$$

Because they are of order $\mathcal{O}(\Delta t^5)$, $\langle F_2^2 \rangle$ and $\langle H_2^2 \rangle$ can be neglected.

[1]J. Miles and D. Henderson, "Parametrically forced surface waves," Annu. Rev. Fluid Mech. **22**, 143 (1990).

[2]T. B. Benjamin and F. Ursell, "The stability of the plane free surface of a liquid in vertical periodic motion," Proc. R. Soc. London Ser. A **225**, 505 (1954).

[3]S. T. Milner, "Square patterns and secondary instabilities in driven capillary waves," J. Fluid Mech. **225**, 81 (1991).

[4]N. B. Tufillaro, R. Ramshankar, and J. P. Gollub, "Order–disorder transition in capillary ripples," Phys. Rev. Lett. **62**, 422 (1989).

[5]S. Douady, S. Fauve, and O. Thual, "Oscillatory phase modulation of parametrically forced surface waves," Europhys. Lett. **10**, 309 (1989).

[6]B. Christiansen, P. Alstrøm, and M. T. Levinsen, "Ordered capillary-wave states: Quasicrystals, hexagons, and radial waves," Phys. Rev. Lett. **68**, 2157 (1992).

[7]S. Fauve, K. Kumar, C. Laroche, D. Beysens, and Y. Garrabos, "Parametric instability of a liquid–vapor interface close to the critical point," Phys. Rev. Lett. **68**, 3160 (1992).

[8]G. Searby and D. Rochwerger, "A parametric acoustic instability in premixed flames," J. Fluid Mech. **231**, 529 (1991).

[9]G. Z. Gershuni and E. M. Zhukhovitskii, *Convective Stability of Incompressible Fluids* (Keter, Jerusalem, 1976).

[10]A. A. Wheeler, G. B. McFadden, B. T. Murray, and S. R. Coriell, "Convective stability in the Rayleigh–Bénard and directional solidification problems: High frequency gravity modulation," Phys. Fluids A **3**, 2847 (1991).

[11]B. V. Saunders, B. T. Murray, G. B. McFadden, S. R. Coriell, and A. A. Wheeler, "The effect of gravity modulation on thermoslutal convection in an infinite layer of fluid," Phys. Fluids A **4**, 1176 (1992); B. T. Murray, S. R. Coriell, and G. B. McFadden, Bull. Am. Phys. Soc. **37**, 1760 (1992).

[12]R. P. Chassay and A. J. Schwaniger, Jr., NASA Tech. Memo. TM 86585 (1986).

[13]E. S. Nelson, "An examination of anticipated *g*-jitter on Space Station and its effects on materials process," NASA Tech. Memo. TM 103775 (1991).

[14]H. U. Walter (editor), *Fluid Sciences and Materials Sciences in Space* (Springer-Verlag, New York, 1987).

[15]J. I. D. Alexander, "Low-gravity experiment sensitivity to residual acceleration: A review," Microgravity Sci. Technol. **3**, 52 (1990).

[16]D. Jacqmin and W. M. B. Duval, "Instabilities caused by oscillating accelerations normal to a viscous fluid–fluid interface," J. Fluid Mech. **196**, 495 (1988).

[17]D. Jacqmin, "Stability of an oscillated fluid with a uniform density gradient," J. Fluid Mech. **219**, 449 (1990).

[18]Y. Zhang and J. I. D. Alexander, "Sensitivity of liquid bridges subject to axial residual acceleration," Phys. Fluids A **2**, 1966 (1990).

[19]J. M. Perales and J. Meseguer, "Theoretical and experimental study of the vibration of axisymmetric viscous liquid bridges," Phys. Fluids A **4**, 1110 (1992).

[20]J. I. D. Alexander, J. Ouazzani, and F. Rosenberger, "Analysis of the low gravity tolerance of Bridgman–Stockbarger crystal growth II. Transient and periodic accelerations," J. Cryst. Growth **113**, 21 (1991).

[21]B. N. Antar, "Thermal instability of stochastically modulated flows," Phys. Fluids **20**, 1785 (1977).

[22]G. H. Fichtl and R. L. Holland, "Simplified model of statistically stationary spacecraft rotation and associated induced gravity environments," NASA Tech. Memo. TM 78164 (1978).

[23]K. D. Ruvinsky, F. I. Feldstein, and G. I. Freidman, "Numerical simulations of the quasi-stationary stage of ripple excitation by steep gravity–capillary waves," J. Fluid Mech. **230**, 339 (1991).

[24]J. Casademunt, W. Zhang, J. Viñals, and R. F. Sekerka, "Stability of a fluid surface in a microgravity environment," AIAA J. (in press).

[25]L. D. Landau and E. M. Lifshitz, *Méchanics* (Pergamon, New York, 1976).

[26]C. M. Bender and S. A. Orszag, *Advanced Mathematical Methods for Scientists and Engineers* (McGraw-Hill, New York, 1978).

[27]C. W. Gardiner, *Handbook of Stochastic Methods for Physics, Chemistry and Natural Sciences* (Springer-Verlag, New York, 1985).

[28]K. Lindenberg and B. J. West, *The Nonequilibrium Statistical Mechanics of Open and Closed Systems* (VCH, New York, 1990).

[29]A. Hernández-Machado and M. San Miguel, "Dynamical properties of non-Markovian stochastic differential equations," J. Math. Phys. **25**, 1066 (1984).

[30]N. G. van Kampen, *Stochastic Processes in Physics and Chemistry* (North-Holland, New York, 1981).

[31]R. L. Stratonovich, *Topics in the Theory of Random Noise* (Gordon and Breach, New York, 1967), Vol. II.

[32]Throughout this paper we take the Stratonovich interpretation of multiplicative white noise (see Ref. 27).

[33]V. E. Shapiro and V. M. Loginov, "The effective potential in a rapidly oscillating irregular field," Phys. Lett. A **71**, 387 (1979); "Erata" **74**, 457 (1979).

[34]V. M. Loginov and V. E. Shapiro, "On delocalization of motions in nonuniform high frequency fields with finite correlation time," Phys. Scr. **21**, 825 (1980).

[35]J. M. Sancho, M. San Miguel, S. L. Katz, and J. D. Gunton, "Analytical and numerical studies of multilplicative noise," Phys. Rev. A **26**, 1589 (1982).

[36]R. Mannella and V. Palleschi, "Fast and precise algorithm for computer simulation of stochastic differential equations," Phys. Rev. A **40**, 3381 (1989); R. F. Fox, "Second-order algorithm for the numerical integration of colored-noise problems," **43**, 2649 (1991).